Toward Selection of a Propulsion Method for a Long Range Benthic Imaging AUV

Daniel Steinberg, Asher Bender, Ariell Friedman
Email: {d.steinberg, a.bender, a.friedman}@acfr.usyd.edu.au
Australian Centre for Field Robotics
School of Aerospace Mechanical and Mechatronic Engineering
University of Sydney, NSW, 2006, Australia

Abstract

The success of underwater gliders in monitoring programs suggests that man-portable autonomous underwater vehicles (AUV) are an amenable size for large-scale monitoring programs from a budgetary and handling perspective. We contend that a man-portable, long-range AUV equipped with a suitable low power optical imaging package may be able to perform cost-effective, long-term monitoring of the benthos, for example to examine the response of sea-floor ecosystems to climate change.

Buoyancy driven gliders achieve a high endurance by operating at low speeds with low hotel loads. Man-portable, propeller-driven AUVs typically operate at high speeds with high hotel loads resulting in relatively low endurance. This paper examines whether one method of propulsion can provide an intrinsic advantage in terms of efficiency at low speed, or whether the present situation is a result of the nature of the data collected by these vehicles.

We employ first-principle analyses to show that either class of vehicle can be designed to achieve the same transit performance regardless of speed. This result implies that the choice of propulsion method should be driven exclusively by the application and operational requirements.

1 Introduction

Australia has over 800,000 km^2 of designated marine protected areas. Programs established to monitor their long-term stability and the response of their benthic ecosystems to climate change have been limited by a lack of systematic and nationwide approaches [1].

Currently, optical surveying of the benthos is done using high power imaging AUVs, remotely operated vehicles (ROVs), manned submersibles, drop cameras, towed systems and human divers. All of these tended survey methods rely on a dedicated, costly support ship.

Imaging AUVs and manned submersibles have the advantage of being de-coupled from surface motions. This allows them to closely follow rough terrain and yields extremely high-quality imagery through consistent altitude and lighting. However, these platforms are limited by their high power requirements. Missions typically last on the order of hours.

Human dive operations are constrained by depth, safety concerns and limited bottom time. Drop cameras and towed video systems can cover broad areas but are heavily reliant on ship availability and are constrained by weather and the ruggedness of the terrain being studied.

Because of high running costs, tended surveys are most economic when they are conducted as quickly as possible. As a result they generally cover small spatial regions with a high intensity.

Detecting long term changes in benthic habitats does not place strict time constraints on the frequency or speed at which surveys are conducted. Cost effective, dense sampling of large marine parks is unfeasible with current technologies, because of their size. To cost effectively obtain representative data sets over these areas surveys will have to be sparse. Given that marine park monitoring is characterised by large-spatial scales, weak temporal requirements and sparse sampling, tended surveys are uneconomic and ill-suited to this task.

This gives rise to a niche for the development of an untended platform designed for long-term monitoring of benthic environments. The success of underwater gliders in monitoring programs [2] suggests man-portable AUVs are an amenable size for monitoring roles from a budgetary and handling perspective. Based on their success, we will focus on man-portable vehicles in this paper.

For untended platforms, the running costs are low compared to the cost of deployment and recovery. As a result, untended surveys are most economic when the number of deployments is minimised. This can be achieved by maximising the range of the untended platform.

The remainder of this paper is organised as fol-

lows. Section 2 states the relationship between hotel power, horizontal velocity and range. A metric for evaluating achievable range per unit of energy, transit performance, is proposed in Section 3. The transit performance of a propeller-driven AUV and glider are derived in Section 4. These first-principle models are compared in Section 5. The results show that propeller-driven AUVs and gliders can be designed to have the same transit efficiency, which is transit performance normalised with respect to an ideal case. Based on this outcome, Section 6 concludes that the choice of propulsion method should be driven exclusively by the application and operational requirements.

2 Propulsion and Range

Range is a function of on-board energy storage, E, propulsive power, P_P, hotel power, P_H, and horizontal velocity, $\dot{x}$. This relationship is given in [3]

$$R = \frac{E}{P_P + P_H} \cdot \dot{x}.$$

Propulsive power is a function of velocity and can be written as

$$P_P = \frac{\rho \dot{x}^3 S C_{DS}}{2\eta}.$$

Where C_{DS} is vehicle drag based on a reference area S, and η is the efficiency of the propulsion system. Since propulsive power is a cubic function of velocity, range reduces with velocity for any given hotel load.

Maximum range can be obtained by differentiating range with respect to propulsive power [3]. The optimal velocity for a given hotel power is then

$$\dot{x} = \sqrt[3]{\frac{\eta P_H}{\rho S C_{DS}}}. \quad (1)$$

Equation 1 shows that it is optimal to operate at a high velocity for a high hotel load. This is so that sufficient survey coverage is obtained before the hotel load exhausts energy reserves.

This is reflected in the operation of REMUS100 which is a man portable AUV. It has been designed for exploratory sampling and has a total power consumption of 45 W. At its nominal speed of 1.5 m/s, REMUS100 has an endurance of 22 hours [4].

The Slocum glider is comparable in size to REMUS100, but it has been designed for taking oceanographic profiles. A low power hotel load, on the order of 1 W [5], allows Slocum to travel at a low velocity, 0.4 m/s [6]. Despite storing only slightly more than twice the energy of REMUS100 [4, 5], Slocum can achieve relatively long ranges and has a typical endurance of 30 days.

It is clear that in order to maximise range, hotel power must be minimised and velocity must satisfy Equation 1. This design specification, paired with the weak temporal and spatial sampling requirements associated with monitoring large-scale marine parks, motivates the need for a new vehicle design.

We will consider both propeller-driven AUVs and gliders as candidates for this new vehicle. For our purposes we believe sampling of the benthos can be performed adequately with each platform. Any sampling limitations introduced by the dynamics of the vehicle can be overcome by intelligent sampling design.

For the remainder of this paper we assume a low power hotel load and focus on the efficiency of propulsion methods at low velocities. In particular, we will determine if there are any compelling reasons to pick a propeller over gliding (or vice versa) for a low velocity transit.

3 The Transit Performance Metric

The purpose of this study is to determine the efficiency of gliders and propeller-driven AUVs as they move between two sample locations. Hence, transit performance will be measured by how many *horizontal* metres these vehicles can travel per joule of energy (m/J).

The aim of this analysis is to uncover which method of propulsion has the best transit performance. Two cases are considered:

1. A propeller-driven AUV
2. A buoyancy-driven autonomous underwater glider

The transit performance measure, Λ, is equivalent to the reciprocal of the horizontal component of the AUVs propulsive force, i.e.

$$Energy = Force \times Distance,$$

so

$$\frac{Distance}{Energy} = \frac{1}{Force},$$

or

$$\Lambda(m/J) = \frac{1}{T_{horiz}(N)}.$$

The transit performance of an AUV with a loss-less propulsion system is derived in Section 4.1. Its purpose is to normalise away the inverse quadratic dependance of transit performance on velocity, which is present in all AUVs. We term this normalised quantity transit efficiency, which takes the following form

$$\eta_{Vehicle} = \frac{\Lambda_{Vehicle}}{\Lambda_{Ideal}}.$$

This form of efficiency only accounts for losses due to the mode of propulsion. Additional losses in the system, such as mechanical and electrical losses, are not included in this definition of efficiency.

The following general assumptions are used for this analysis:

1. All the AUVs compared have an equivalent hull design and hull drag coefficient. Volume devoted to energy stores, propulsion and control hardware is the same in each AUV. Furthermore the hotel and sensing loads are equivalent as the mission requirements are the same.

2. Any non-steady accelerating motions are assumed to occupy a negligibly small fraction of the total mission time, hence only steady motions are considered for the purpose of this analysis. Consequently, straight line transit is assumed, i.e. no turning motions are considered.

3. The propeller-driven and ideal AUVs are neutrally buoyant, and sea water exhibits a constant density.

Propeller-driven AUVs are usually slightly positively buoyant as a fail safe. To overcome their buoyancy and local variations in sea water density, these AUVs make use of control surfaces or actuators. Normally these techniques introduce additional drag due to lift from the hull and control surfaces at non zero angles of attack [3]. In our analysis we ignore this effect and assume neutral buoyancy. This remains a practical challenge but may be possible by installing a small buoyancy control system on the vehicle.

4 Transit Performance

In this section the transit performance metrics are derived from first principles for propeller-driven AUVs and gliders. Using these models we aim to uncover any velocity dependence that would indicate one method of propulsion is superior to the other for low speed transit. We show that neither of the models are dependent on velocity.

4.1 Ideal Propulsion

An AUV with a loss-less propulsion system will have perfect transit efficiency for the selected hull shape. This vehicle is presented to normalise the transit performance of the propeller-driven AUV and glider.

From Figure 1, it can be seen that for a steady horizontal velocity, thrust must equal drag

$$T = \frac{1}{2}\rho S_h \dot{x}^2 C_{Dh}, \tag{2}$$

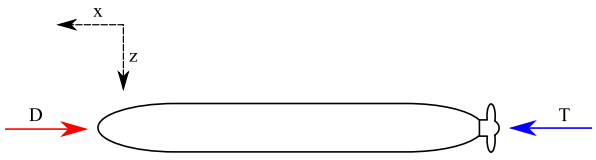

Figure 1: Free body diagram (FBD) of an AUV with loss-less propulsion

where S_h is the AUV hull frontal area, C_{Dh} is the AUV's drag coefficient referenced to S_h, and ρ is the fluid density. Hence

$$\Lambda_{Ideal} = \frac{1}{T} = \frac{2}{\rho S_h \dot{x}^2 C_{Dh}}. \tag{3}$$

4.2 Propeller-Driven AUV

Momentum theory can be used to model the performance of a propeller. Although momentum theory does not account for fluid rotation in the slipstream or energy lost to viscous drag, it is an attractive model because propeller geometry can be expressed with one design parameter. The ideal propulsive efficiency of an actuator disk, η_{AD}, predicted by momentum theory is given by [7]

$$\eta_{AD} = \frac{2}{1 + \left(\frac{2T}{\rho S_p \dot{x}^2} + 1\right)^{\frac{1}{2}}}.$$

Where S_p is the area of the actuator disk. Since the thrust, T, produced by the actuator disk must overcome hull drag (Equation 2), the efficiency of the propeller-driven AUV can be restated as

$$\eta_{AD} = \frac{2}{1 + \left(C_{Dh} f_p^{-2} + 1\right)^{\frac{1}{2}}}. \tag{4}$$

Where the propeller diameter ratio, $f_p = d_p/d_h$, defines the ratio between the actuator disk diameter, d_p, and the hull diameter, d_h.

A propeller cannot perfectly translate energy into motion. Since the energy supplied to an actuator disk is reduced by the efficiency of the actuator disk, the transit performance for the propeller-driven AUV can be written as

$$\Lambda_{AD} = \frac{\eta_{AD}}{T}.$$

If transit performance is normalised by the ideal propulsion scheme (Equation 3), the transit efficiency of the propeller-driven AUV is simply the efficiency of the actuator disk (Equation 4)

$$\frac{\Lambda_{AD}}{\Lambda_{Ideal}} = \eta_{AD}.$$

For a given hull design, the transit efficiency of a propeller-driven AUV is only a function of the propeller diameter ratio. An outcome of this result, is that transit efficiency is independent of horizontal velocity.

4.3 Autonomous Underwater Glider

A typical glider configuration uses a buoyancy engine and symmetric wings to translate buoyancy into lift, effectuating horizontal motion. Figure 2 shows the forces acting on the glider in the longitudinal plane.

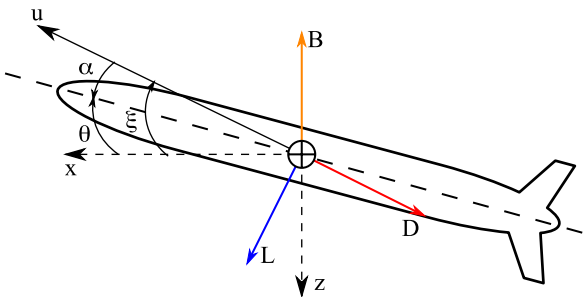

Figure 2: FBD of the forces acting on a glider in the longitudinal plane

Only the longitudinal plane of motion is considered in the transit performance model, so it is necessary to resolve the lift and total drag forces to the horizontal (x) axis. Using Figure 2, the horizontal forces can be determined from $\sum F_x = 0$

$$0 = L\sin\xi - D\cos\xi$$
$$L\sin\xi = D\cos\xi$$

Here ξ is the glide path angle and $L\sin\xi$ and $D\cos\xi$ are equivalent to the horizontal propulsive force. Transit performance is given by their inverse

$$\Lambda_G = \frac{1}{L\sin\xi} = \frac{1}{D\cos\xi}.$$

Drag has parasitic and lift-induced components, so for simplicity, we will use $\frac{1}{L\sin\xi}$. Substituting for L,

$$\Lambda_G = \frac{2}{\rho u^2 S_w C_{Lw}\alpha\sin\xi}. \tag{5}$$

Here C_{Lw} is the wing lift coefficient referenced to wing planform area, S_w. Velocity along the glide path is u, and α is the angle of attack.

An equation for angle of attack is derived in [8]. To reduce the dimensionality of this equation, we assume that there is no parasitic wing drag, C_{Dw}. Furthermore the Oswald Efficiency Factor of the wing, e, is assumed to be 1. That is, the wing geometry perfectly utilises the lift distribution along the wing. With these assumptions, angle of attack is

$$\alpha = \frac{\pi A}{2C_{Lw}}\tan\xi\left(1 - \sqrt{1 - C_{Dh}f_b^{-2}\cot^2\xi}\right), \tag{6}$$

where A is the wing's aspect ratio and the wingspan ratio, $f_b = b/d_h$, defines the ratio between the wingspan, b, and hull diameter, d_h.

Parasitic drag has hull *and* wing drag components, so the assumption of $C_{Dw} \approx 0$ will lead to an underestimation of drag and overestimation of lift. Assuming an Oswald efficiency of 1 will have a similar effect.

Substituting $u = \dot{x}/\cos\xi$ and Equation 6 into Equation 5 yields

$$\Lambda_G = \frac{4\cot^2\xi\cos\xi}{\rho\dot{x}^2\pi S_w A\left(1 - \left(1 - C_{Dh}f_b^{-2}\cot^2\xi\right)^{\frac{1}{2}}\right)} \tag{7}$$

where glide angle is subject to bounds dictated by stall. This hydrodynamic model is only accurate for small angles of attack [8].

4.3.1 Normalise With Respect to Ideal

After normalising the glider transit performance (Equation 7) with respect to the ideal transit performance (Equation 3), we obtain

$$\eta_G = \frac{C_{Dh}f_b^{-2}\cot^2\xi\cos\xi}{2\left(1 - \left(1 - C_{Dh}f_b^{-2}\cot^2\xi\right)^{\frac{1}{2}}\right)}. \tag{8}$$

The glider transit efficiency model, Equation 8, shows that the transit efficiency of the glider is independent of horizontal velocity, $\dot{x}$, and wing planform area S_w.

4.3.2 Optimal Glide-path Angle

Figure 3 shows the transit performance of Slocum with respect to glide-path angle. Transit efficiency, η_G, is maximised at a glide-path angle of 18°. In general, the optimum glide-path angle can be found as a function of f_b and C_{Dh}. This can be used to reduce the parameter space of Equation 8.

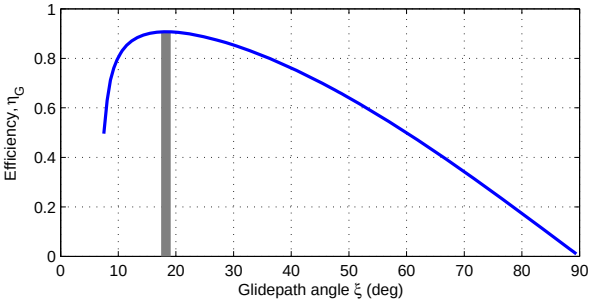

Figure 3: Glider efficiency vs. glide angle for the Slocum. The optimal glide-path angle is $\xi_{Opt} = 18°$ using the parameters specified in Table 1.

By setting $\frac{\delta\eta_G}{\delta\xi} = 0$ and solving for ξ, we get the following equation for the optimal glide-path angle

$$\xi_{Opt} = \pm\tan^{-1}\left(\frac{1}{3}\left(Q + 4\left(C_{Dh}f_b^{-2}\right) - 2 + \frac{20\left(C_{Dh}f_b^{-2}\right) + 16\left(C_{Dh}f_b^{-2}\right)^2 + 4}{Q}\right)^{\frac{1}{2}}\right) \tag{9}$$

where

$$Q = \left(\frac{123}{2} \left(C_{Dh} f_b^{-2} \right) + 120 \left(C_{Dh} f_b^{-2} \right)^2 + 64 \left(C_{Dh} f_b^{-2} \right)^3 - 8 + 18 \left(-6 \left(C_{Dh} f_b^{-2} \right) - \frac{183}{16} \left(C_{Dh} f_b^{-2} \right)^2 - 6 \left(C_{Dh} f_b^{-2} \right)^3 \right)^{\frac{1}{2}} \right)^{\frac{1}{3}}.$$

This result shows that the optimal glide path angle is independent of the vehicle's velocity. Consequently, for a given hull design, glider transit efficiency is only a function of f_b.

5 Results

We have previously shown that transit efficiency has no dependence on velocity and that each model has been distilled down to one design parameter. We show that it is possible to use either design to attain the same transit efficiency. In this section we explore the nuances of these models and practical issues.

The parameters used to generate the transit performance and efficiency for REMUS100 [9] and Slocum [10, 11] are given in Table 1.

Table 1: Parameters for the Slocum and REMUS100 AUVs

Parameter	Slocum	REMUS100
C_{Dh}	0.4305	0.267
S_h m^2	0.034	0.028
Design Ratios	$f_b = 4.8077$	$f_p = 0.7353$

5.1 Propeller-Driven AUV Results

Figure 4 summarises the transit efficiency for a propeller-driven AUV, η_{AD}, as a function of propeller diameter ratio, f_p.

The transit efficiency of a propeller-driven AUV can be improved by increasing its propeller diameter ratio. However, improvements to efficiency diminish as propeller diameter ratio increases, particularly at lower drag coefficients.

5.2 Glider Results

Figure 5 summarises the transit efficiency for a glider, η_G, as a function of the wingspan ratio, f_b. It is evident that a larger wingspan ratio provides higher transit efficiency, which is consistent with results the presented in [10].

Improvements to transit efficiency, however, occur at a diminishing rate, which is particularly prevalent for low drag coefficients. As a result, significant gains to transit efficiency obtained by increasing the wingspan ratio, are harder to achieve for lower drag designs.

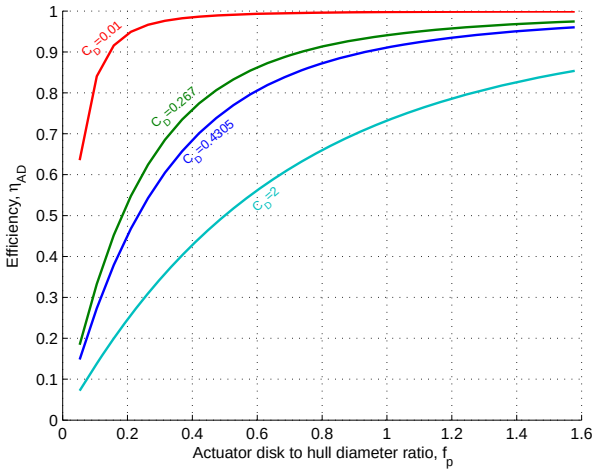

Figure 4: Efficiency of an propeller-driven AUV with varying propeller diameter ratios, f_p for selected drag coefficients

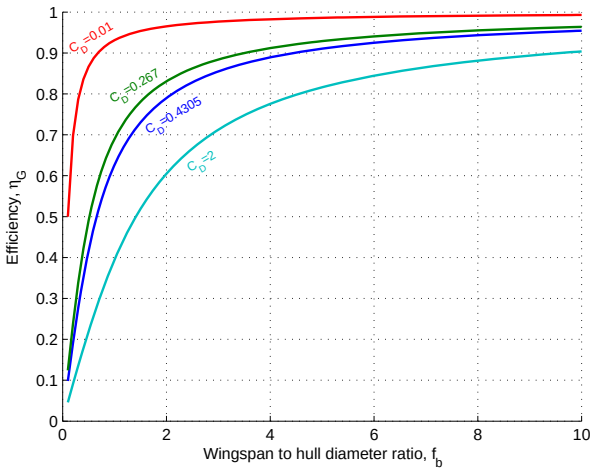

Figure 5: Efficiency vs. wingspan ratio for selected drag coefficients

Figure 6 shows how the optimal glide-path angle changes with the wingspan ratio for selected drag coefficients. As the wingspan ratio increases the glide-path angle becomes shallower. Furthermore, a glider with a low coefficient of drag will transit at a relatively shallow glide-path angle.

The glider model derived in this paper implies that transit efficiency is independent of aspect ratio, A. This is also true for transit performance since the $S_w A$ term in the denominator of Equation 7 is equivalent to wing span squared (b^2). As a result, the parameter f_b does not fully specify the shape of the wing. According to our analysis a glider with a low aspect ratio (wide wing) will have an equivalent transit efficiency to a glider with a high aspect ratio (slender wing) of the same hull design. Because the effects of parasitic wing drag

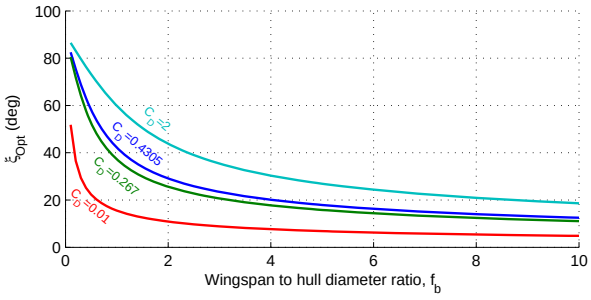

Figure 6: Optimal glide-path angle vs. wingspan ratio for selected drag coefficients

are omitted from the model, there is no penalty associated with large wing planform area, for a given wingspan ratio.

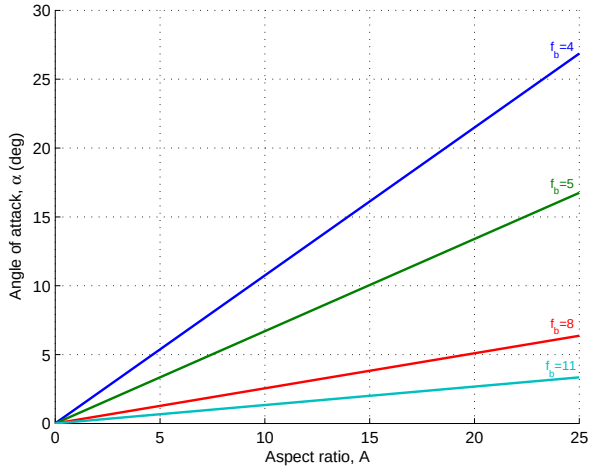

Figure 7: Angle of attack vs. aspect ratio for selected wingspan ratios. The Slocum drag coefficient from Table 1 is used.

The relationship between angle of attack, α, and aspect ratio, A, given by Equation 6 is depicted in Figure 7. A low angle of attack is desirable for two reasons. Firstly, the hydrodynamic models in this paper are only accurate for small angles of attack. This places a limit on the slenderness of wings for this model to be accurate. This is particularly true for low wingspan ratios. Secondly, while operating with large angles of attack, induced drag due to the wings and hull will reduce transit efficiency. This effect is not explicitly taken into account by this model, but is an important practical consideration.

It can be seen from Figure 7 that when applied to small angles of attack and large wingspan ratios, our model allows for high aspect ratios. This produces a wing geometry resembling that of sailplanes.

5.3 Comparison of Transit Performance

The vehicle design parameters f_p and f_b can be varied so that a propeller-driven AUV and a glider have the same transit efficiency. The exact relation between these design parameters can be found by equating the transit efficiencies given by Equation 4 and Equation 8 to yield

$$f_p = \frac{C_{Dh}^{\frac{1}{2}}}{\sqrt{\left(\frac{4\left(1-\sqrt{1-C_{Dh}f_b^{-2}\cot^2\xi_{Opt}}\right)}{C_{Dh}f_b^{-2}\cot^2\xi_{Opt}\cos\xi_{Opt}}-1\right)^2-1}}. \tag{10}$$

Equation 10 states propeller diameter ratio as a function of wingspan ratio and hull drag coefficient (where $\xi_{Opt} = f(f_b, C_{Dh})$). This relation specifies an equally efficient propeller-driven AUV configuration for a given glider configuration.

Figure 8 is a graphical representation of the relationship derived in Equation 10 for a range of drag coefficients and design parameters. The solid curves represent equivalent transit efficiencies for a constant drag coefficient. A point on these curves provides the design parameters f_p and f_b that will produce the same transit efficiency for a given drag coefficient. The dotted lines show constant transit efficiency across all drag coefficients.

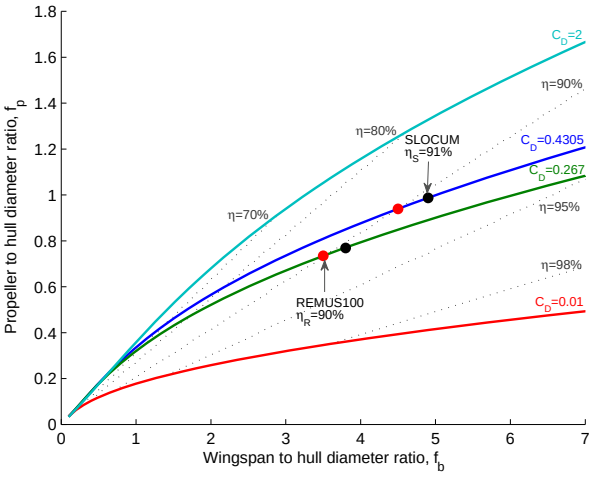

Figure 8: Span ratio, f_b, vs. propeller diameter ratio, f_p, for equal transit efficiency. Points for a glider (red) and a propeller-driven AUV (black) have been shown which correspond to designs with the same transit efficiency as the REMUS100 and Slocum respectively.

For the purpose of relating these results to realistic designs, the positions of REMUS100 and Slocum have been highlighted on the plot. This does not imply that these vehicles will be used for long range benthic surveying.

Table 2 shows the parameters for propeller-driven AUVs and gliders with transit efficiencies of 90%,

Table 2: Summary of selected points from Figure 8

Vehicle	η	C_{Dh}	d_h	Design Parameter	Dimensional Parameter
REMUS100	90%	0.267	19 cm	$f_p = 0.7353$	$d_p = 14.0$ cm
Prop-AUV1	91%	0.267	19 cm	$f_p = 0.769$	$d_p = 14.6$ cm
Prop-AUV2	95%	0.267	19 cm	$f_p = 1.104$	$d_p = 21.0$ cm
Glider-AUV1	90%	0.4305	20.8 cm	$f_b = 4.5$	$b = 0.94$ m
Slocum	91%	0.4305	20.8 cm	$f_b = 4.9$	$b = 1.02$ m
Glider-AUV2	95%	0.4305	20.8 cm	$f_b = 9.1$	$b = 1.89$ m

91% and 95%. This table shows that REMUS100 and Slocum have similar transit efficiencies in their original configurations, according to our models.

To obtain an equivalent transit efficiency to Slocum, REMUS100 would need a propeller diameter ratio of $f_p \approx 0.77$. This is a propeller diameter of approximately 14.6 cm rather than its standard propeller diameter of 14 cm [9]. For Slocum to exhibit the same efficiency as REMUS100, it would require a span ratio of about 4.5 ($b \approx 0.94$ m) rather than its current value of approximately 5 ($b \approx 1$ m). These changes are minimal.

To reach a transit efficiency of 95%, REMUS100 would require a propeller diameter of $d_p = 21.0$ cm, which is an increase of 50% on the standard propeller size. For Slocum, a wingspan of about 1.9 m would be required. This represents an increase of over 85% on the original wingspan.

This comparison and Figure 8 show that the wingspan ratio has to be increased proportionally more than the propeller diameter ratio to achieve the same gain in transit efficiency. This effect is greater for low drag coefficients.

This study has shown that neither propeller-driven AUVs nor gliders have any advantage over the other. This is because they can be designed to achieve the same transit efficiency. This result implies that the choice of propulsion method should be driven exclusively by the application and operational requirements.

6 Conclusion

The monitoring of large scale marine protected areas requires autonomous vehicles to traverse large distances. Hypothetically, an AUV equipped with a low power imaging sensor would be able to travel at a low velocity, resulting in a high transit efficiency. From propulsion considerations alone, our analysis shows that propeller-driven AUVs and gliders can be designed to achieve the same transit performance regardless of velocity.

Given that each platform can be designed to achieve a target transit efficiency, when designing a vehicle for long range transit, our models imply the choice of propulsion method is dependent on the application and practical considerations.

This outcome can be extended to hybrid vehicles. Given that no platform offers superior transit performance, there are no optimal characteristics to combine. Thus, a hybrid glider system that incorporates a buoyancy engine, wings and thrusters will require more volume for hardware, reducing energy storage capacity for no realisable advantage in transit performance.

These conclusions must be viewed in light of the assumptions we have made. By excluding the effect of parasitic drag on the wings and propeller blades, no penalty to transit efficiency is placed on their surface areas. Including the effects of parasitic drag may exclude one platform from operating efficiently in a low velocity regime as parasitic drag has a Reynolds number dependancy. Work is being done to extend these models and relax some of their simplifying assumptions.

Based on the outcomes of our analysis, we recommend a propeller-driven AUV for large scale marine park monitoring. Level flights above the benthos, will not place any constraints on the sampling strategy and make propeller driven AUVs a more practical choice than gliders. The marine robotics division of the Australian Centre for Field Robotics (ACFR) is developing this concept and hopes to produce a working prototype. This prototype will help marine biologists observe the effects of climate change on our precious underwater ecosystems.

7 Acknowledgements

The authors wish to acknowledge the encouragement, insight, and comprehensive critiques provided by Michael Jakuba, Oscar Pizarro and Stefan Williams of the ACFR.

This work is supported by the Australian Research Council (ARC) Centre of Excellence programme and funded by the New South Wales State Government.

References

[1] "A national approach to addressing marine biodiversity decline," Marine Biodiversity Decline Workgroup, April 2008, a report to the Natural Resource Management Ministerial Council.

[2] O. Schofield, J. Kohut, H. Roarty, S. Glenn, C. Jones, and D. Webb, "Enabling discovery based science with webb gliders," *US/EU-Baltic International Symposium, 2008 IEEE/OES*, pp. 1–6, May 2008.

[3] M. Furlong, S. McPhail, and P. Stevenson, "A concept design for an ultra-long-range survey class auv," *OCEANS 2007 - Europe*, pp. 1–6, June 2007.

[4] "Remus 100 specification," http://www.hydroidinc.com/100spec.html, Hydroid, Accessed 29/3/2009.

[5] R. E. Davis, C. C. Eriksen, and C. P. Jones, "Autonomous bouyancy-driven underwater gliders," in *The Technology and Applications of Autonomous Underwater Vehicles*, G. Griffiths, Ed. London: Taylor and Francis, 2002.

[6] "Electric glider," http://www.webbresearch.com/electricglider.aspx, Teledyne Webb Research, Accessed 1/4/2009.

[7] J. P. Ghose and R. P. Gokarn, *Basic Ship Propulsion*. Allied Publishers, 2004.

[8] J. G. Graver, "Underwater gliders: Dynamics, control and design," PhD, Princeton University, 2005.

[9] B. Allen, W. Vorus, and T. Prestero, "Propulsion system performance enhancements on remus auvs," *OCEANS 2000 MTS/IEEE Conference and Exhibition*, vol. 3, pp. 1869–1873 vol.3, 2000.

[10] J. Sherman, R. E. Davis, W. B. Owens, and J. Valdes, "The autonomous underwater glider 'spray'," *IEEE Journal of Oceanic Engineering*, vol. 26, no. 4, 2001.

[11] J. S. Geisbert, "Hydrodynamic modeling for autonomous underwater vehicles using computational and semi-empirical methods," Masters, Virginia Polytech Institute and State University, 2007.